(Takara) with primers described previously (Tachibana *et al.* 2007). The phosphoglucomutase (PGM) gene was amplified using the primers 5′-TCG TTG AAC CAG ATC AGT GC-3′ and 5′-AAG CTT CTC TGG ATG GTG TTG-3′, as described in Takano *et al.* (2009). The PCR conditions using PrimeSTAR HS DNA polymerase were as follows: denaturation at 98 °C for 10 s, annealing at 55 °C (for *HXK* and *GPI*) or 60 °C (for *PGM*) for 5 s, and extension at 72 °C for 90 s.

Sequencing

PCR products of rRNA genes, serine-rich protein genes, and *PGM* genes were subjected to direct sequencing after purification using a QIAquick PCR purification kit (Qiagen). PCR products of the *HXK* and *GPI* genes were processed with a Zero Blunt TOPO PCR cloning kit for sequencing (Invitrogen). Six clones of each gene were sequenced using a BigDye Terminator v3.1 Cycle Sequencing kit (Applied Biosystems). The reactions were run on an ABI Prism 3100 Genetic Analyzer (Applied Biosystems).

Zymodeme analysis

Isoenzyme analysis of cultured trophozoites in starch gel was performed using a literature method (Sargeaunt, 1988), with determination of the mobilities of 4 enzymes: HXK, GPI, PGM, and L-malate:$NADP^+$ oxidoreductase (ME).

Hepatic inoculation

Five male Syrian hamsters (*Mesocricetus auratus*) weighing 95–110 g were purchased from Japan SLC, Inc. The hamsters were anaesthetized by intraperitoneal injection of pentobarbital and then 5×10^5 trophozoites cultured axenically were inoculated into the left lobe of the liver. The hamsters were sacrificed 7 days after inoculation and formation of amoebic liver abscesses was examined. Representative liver samples including abscesses were fixed with 4% paraformaldehyde in phosphate buffer and embedded in paraffin. Sections were stained with haematoxylin and eosin (H&E) and PAS (periodic acid-Schiff), and examined by standard light microscopy (Olympus BX51).

Electron microscopy

Small pieces of liver close to an abscess were fixed in periodate/lysine/ paraformaldehyde (PLP) (McLean and Nakane, 1974) overnight at room temperature. The samples were washed with 0·1 M phosphate buffer (pH 7·4), post-fixed with 1% OsO_4 in 50 mM phosphate buffer for 1 h at 4 °C, and then dehydrated with a graded ethanol series and embedded in Quetol 812 (Nisshin EM). Ultrathin sections were stained with uranyl acetate and lead citrate and then examined using a JEOL JEM-1200 EX II transmission electron microscope.

RESULTS

Detection of amoebae by stool examination and PCR

The thirty stool samples were all formed, and not loose, watery or bloody. Cysts of *E. histolytica/ E. dispar/E. nuttalli*, *E. chattoni* and *E. coli* were highly prevalent in microscopic observation. PCR amplification using primers specific for *E. nuttalli* yielded products from all samples, whereas no samples gave products using primers for *E. histolytica* and *E. dispar*. *E. chattoni* and *E. coli* were detected by PCR in all samples and the amplicons were confirmed to be from the expected species by sequencing. Examination of the 30 fecal samples using an *E. histolytica* antigen detection kit gave no positive results.

Isolation of E. nuttalli *in culture*

Growth of trophozoites in Tanabe-Chiba medium was observed in 4 samples. After several passages, *E. nuttalli* DNA was detected by PCR in these samples, but *E. chattoni* and *E. coli* DNA was not amplified. Three of the 4 samples were used as xenic strains and labelled as NASA821, NASA823 and NASA829 for subsequent experiments. One isolate, named the NASA6 strain, was axenized and then cloned. The living trophozoites in the *E. nuttalli* NASA6 strain had an elongated shape of length 18–60 μm. The average diameter of chilled trophozoites of the NASA6 strain ($22{\cdot}4 \pm 0{\cdot}43$ (mean ± S.E.) μm) was significantly smaller than that of the *E. histolytica* HM-1:IMSS strain ($28{\cdot}3 \pm 0{\cdot}54\,\mu$m, $P<0{\cdot}0001$), but larger than that of the *E. nuttalli* P19-061405 strain ($20{\cdot}7 \pm 0{\cdot}29\,\mu$m, $P=0{\cdot}001$). Trophozoites of the NASA6 strain cultured axenically gave a positive result with an *E. histolytica* II antigen detection kit.

Analysis of ribosomal RNA genes in the isolates

The 18S rRNA gene of a clone of the NASA6 strain (DDBJ, EMBL, and GenBank Accession number AB485592) showed 2 nucleotide differences compared with the P19-061405 strain (AB282657), but was identical to the EHMfas1 strain (AB197936). There were no differences in the 5·8S rRNA gene and the internal transcribed spacer (ITS) 1 and 2 regions among the 3 strains. The sequences of the rRNA genes from the 3 xenic isolates were also identical to that of the NASA6 strain.

Analysis of the serine-rich protein gene

The deduced amino acid sequence from the serine-rich protein gene of the NASA6 strain

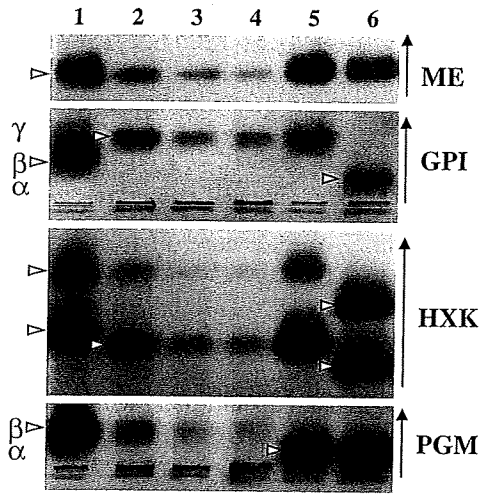

Fig. 1. Isoenzyme patterns for ME, GPI, HXK and PGM of *Entamoeba nuttalli* strains obtained from Japanese macaques (lanes 2 to 4). Lane 1, *E. histolytica* SAW1453 (Zymodeme XIV); lane 2, *E. nuttalli* NASA6 (axenic); lane 3, *E. nuttalli* NASA821; lane 4, *E. nuttalli* NASA829; lane 5, *E. nuttalli* P19-061405; lane 6, *E. dispar* SAW1734RclAR (Zymodeme I). Vertical arrows indicate the direction of migration. Arrowheads indicate positions of bands.

(AB485593) differed from those of the P19-061405 (AB282662) and EHMfas1 (AB197935) strains. In the NASA6 strain, the amino acid motifs EKASSSDKP(cca), EASSN(aat)DKP and EASSSDKS(tca) were present instead of EKASSSDKS(tca), EASSS(agt)DKP and EASSSDKP (cca), respectively, in the P19-061405 and EHMfas1 strains, resulting in single nucleotide substitutions. In addition, the ESSSN(aat)DKP motif was found in the NASA6 strain, for which ESSSS(agt)DKP is the closest sequence motif in human isolates. The sequence in the region with glutamic and aspartic acids in the NASA6 strain was similar to that in EHMfas1, but insertion of an additional ED was found in NASA6. The sequences of serine-rich protein genes in the 3 xenic strains were identical with that of the NASA6 strain, suggesting that only 1 type of *E. nuttalli* was prevalent in the monkeys in the corral.

Analyses of isoenzyme patterns

The electrophoretic patterns of 4 enzymes from the axenic strain (NASA6) and xenic strains (NASA821 and NASA829) of *E. nuttalli* isolated from Japanese macaques are shown in Fig. 1. The patterns for HXK and GPI were identical to those observed in the *E. nuttalli* P19-061405 strain and differed from those of *E. histolytica* and *E. dispar*. However, the mobility of the PGM band in the 3 NASA strains was identical with that in *E. histolytica*, whereas the mobility of this band in the P19-061405 strain was identical with that in *E. dispar*.

Analyses of HXK, GPI *and* PGM *genes*

The calculated molecular mass and theoretical p*I* of HXK1 (AB485594) in the *E. nuttalli* NASA6 strain were 49·8 kDa and 5·38, respectively, and those for HXK2 (AB485595) were 49·3 kDa and 4·99, respectively, with both enzymes containing 445 amino acids. These p*I* values were identical to those for the *E. nuttalli* P19-061405 strain (AB282663 and AB282664), although HXK1 and HXK2 differed by 1 and 2 amino acids, respectively: Ala^{75} in both enzymes in NASA6 compared to Pro^{75} in P19-061405, and Ile^{232} in HXK2 in NASA6 compared to Val^{232} in P19-061405. The amino acid sequences of GPI1 (AB485596) and GPI2 (AB485597) in the *E. nuttalli* NASA6 strain were consistent with the calculated molecular mass of 61·4 kDa and theoretical p*I* of 6·6. These values were also identical to those of the P19-061405 strain (AB282665 and AB282666). Each protein had a single amino acid change from NASA6 to P19-061405: Ile^{232} to Val^{232} in GPI1, and Ala^{330} to Val^{330} in GPI2. *PGM* genes from *E. nuttalli* NASA6 and P19-061405 strains (AB485598 and AB485599) encoded proteins of 553 amino acids with calculated molecular masses of 60·8 kDa. Amino acid differences were detected in 2 positions: Asn^{416} and Asp^{441} in NASA6 compared to Ser^{416} and Asn^{441} in P19-061405. There were 4 differences in amino acids between NASA6 and *E. histolytica* (CAA74796), and 11 differences between NASA6 and *E. dispar* (CAA74797). The p*I* values of PGM from the NASA6 and P19-061405 strains, 5·87 and 5·99, were identical to those from *E. histolytica* and *E. dispar*, respectively.

Virulence in hamsters

Of the 5 hamsters that received intrahepatic inoculation of trophozoites of the NASA6 strain, 1 died at 6 days after inoculation and another died at 7 days after inoculation. In these hamsters, the abscess weights as a percentage of the whole liver were 30% and 35%, respectively, and trophozoites were found in the abscesses in both animals. The other 3 hamsters were sacrificed at 7 days after inoculation and amoebic liver abscesses were also found in these animals. Histopathological analysis of the liver damage produced by *E. nuttalli* trophozoites showed large and irregular necrotic areas of liver parenchyma. These areas were peripherally limited by abundant live and pleomorphic trophozoites associated mainly with chronic inflammatory infiltrates (Fig. 2), forming palisade bands of epithelioid cells with evidence of a granulomatous reaction. The necrotic

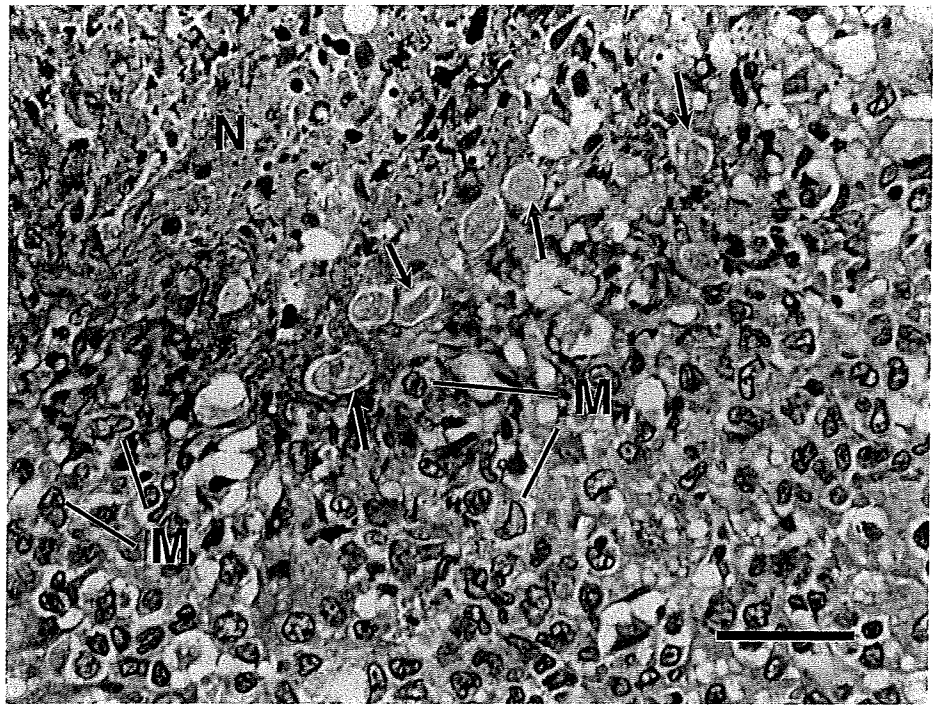

Fig. 2. Liver histology in hamsters inoculated with 5×10^5 trophozoites of the *Entamoeba nuttalli* NASA6 strain. At 7 days after inoculation, areas of necrosis (N) appeared that were limited peripherally by multiple trophozoites (arrows) and mononuclear (M) inflammatory cells. (H&E stain, Scale bar = 40 μm).

zones contained homogeneous and eosinophilic material with cell remnants and dense basophilic deposits.

Electron microscopy of hamster liver inoculated with E. nuttalli *trophozoites*

Electron microscopy of hepatic tissues taken from the vicinity of abscess walls at 7 days after inoculation showed the presence of elongated and pleomorphic trophozoites of *E. nuttalli* that were randomly spread at the outer limits of the abscess. The parasites were surrounded by abundant necrotic tissue formed by hepatic and inflammatory cell remnants composed of small vesicles and dense granules, membrane fragments and damaged cells (Fig. 3A). Some of these cells were partially damaged hepatocytes with cytoplasm containing multiple vesicles, lipid droplets and dilated organelles. Other damaged cells that were closely associated with the parasites and compatible with lysed inflammatory cells are shown in Fig. 3B. These irregularly outlined damaged cells surrounding the trophozoite contained only a fine granular material with a few dense granules distributed mainly at the periphery. Some trophozoites showed initial endocytic activity of damaged cells characterized by concavity at one pole of the parasite associated with an unrecognized damaged cell (Fig. 3B). The nuclei of the trophozoites were round but slightly irregular, and sometimes had an undulating profile (Fig. 3A). Dense chromatin was distributed at the periphery close to the nuclear membrane. The plasma membrane of each trophozoite was intact, thin and sharply defined. The cytoplasm included multiple phagocytic vacuoles of different sizes, with some containing membranous, amorphous or microvesicular material or other cell remnants (Fig. 3A and B). Geometrically arranged crystalloid structures were occasionally observed and glycogen particles were scarce.

DISCUSSION

This study is the first report of isolation of *E. nuttalli* from Japanese macaques. Since *E. nuttalli* was detected in all fecal samples, Japanese macaques appear to be highly susceptible to *E. nuttalli* infection, as well as to *E. coli* and *E. chattoni*. Surprisingly, *E. dispar* was not detected, whereas our previous studies have demonstrated that *E. dispar* is prevalent in Japanese macaques (Rivera and Kanbara, 1999; Tachibana *et al.* 2001). This suggests that the amoeba species prevalent in captive macaques may vary in each colony and may be different from that of wild macaques. The Japanese macaque (*M. fuscata*) is phylogenetically closer to rhesus monkey (*M. mulatta*) than cynomolgus monkey (*M. fascicularis*) (Hayasaka *et al.* 1996; Chu *et al.* 2007), but the sequence of the 18S rRNA gene of the NASA6 strain differed from that of the P19-061405 strain isolated from a rhesus monkey but was identical to that of the EHMfas1 strain isolated from a cynomolgus

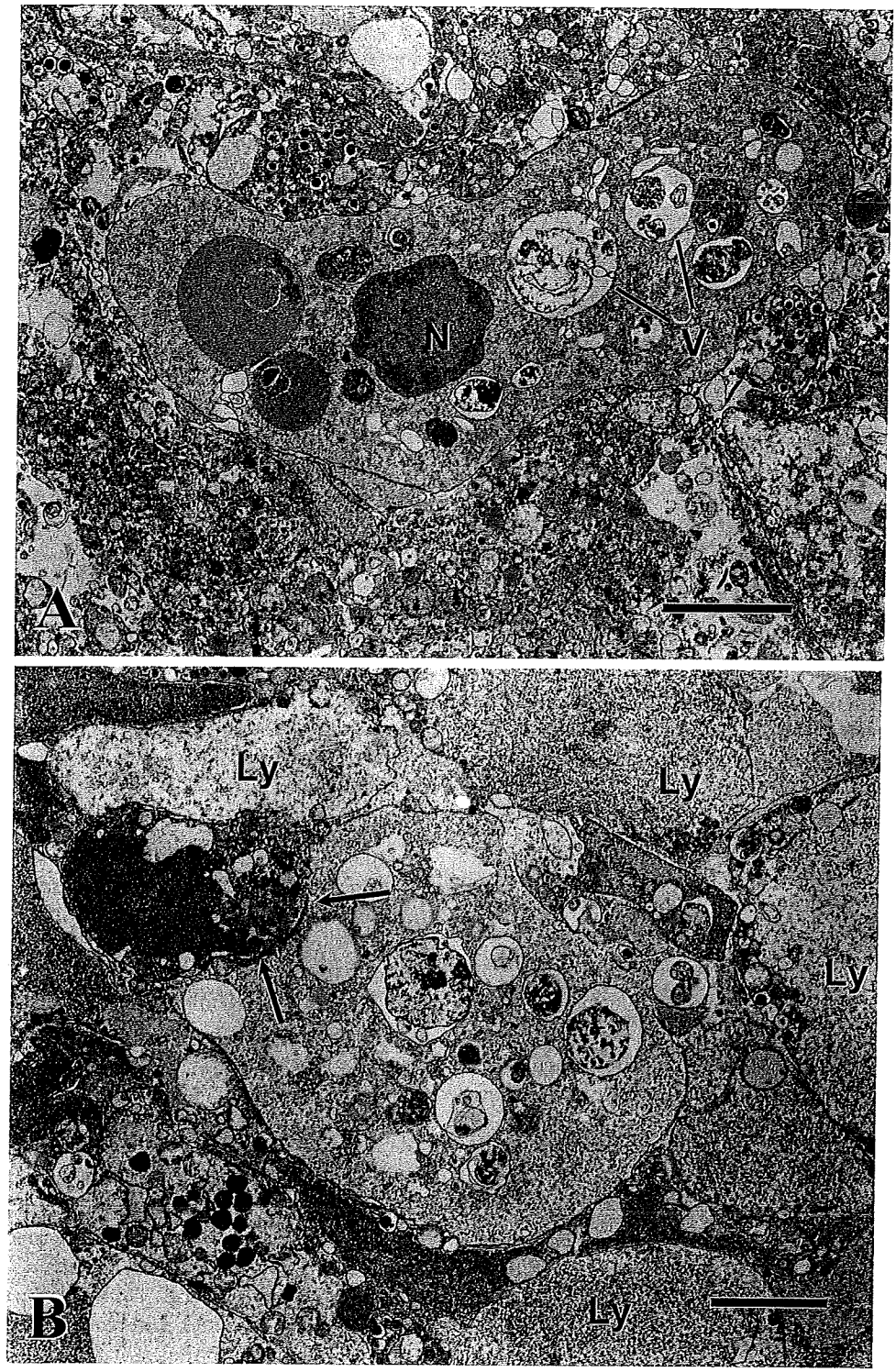

Fig. 3. Transmission electron micrographs of hamster liver at 7 days after inoculation of *Entamoeba nuttalli* NASA6 trophozoites. (A) The image shows an irregularly elongated trophozoite with a round nucleus (N) with peripherally distributed chromatin and a cytoplasm containing multiple vacuoles (V) enclosing membranous or amorphous material and granules of unknown origin. The thin, sharp and intact plasma membrane of the amoeba is apparent. The parasite is surrounded by abundant damaged host cells. (B) The image shows an ovoid trophozoite of *E. nuttalli* in the initial stage of the endocytic process (arrows) with a damaged cell contacting the left pole of the cell. The cytoplasm of the parasite contains vacuoles of different sizes containing unknown material. Multiple lysed (Ly) cells containing a fine granular material with small dense granules are seen surrounding the amoeba. (Scale bar = 3 μm).

monkey. At present, the number of *E. nuttalli* isolates is insufficient to establish the relationship of evolution and dispersal in hosts and parasites, but the NASA6 and EHMfas1 strains clearly differ based on the serine-rich protein gene sequences and isoenzyme patterns.

In zymodeme analysis, the location of the slower running band for HXK and the appearance of a single γ band for GPI may be unique characteristics of *E. nuttalli*-type amoebae, compared with *E. histolytica* and *E. dispar*. In contrast, the pattern for PGM was distinctly different in NASA strains compared with other *E. nuttalli*-type strains in zymodeme analysis, with a β band in the NASA strains and an α band in the other strains. Sargeaunt has suggested that the absence of an α band and the presence of a β band for PGM are characteristics of *E. histolytica* that distinguish it from *E. dispar*, with the exception of zymodeme XIII (Sargeaunt, 1988). NASA6 was the first strain showing *E. histolytica*-type mobility for PGM, while the P19-061405, EHMfas1 and JSK2004 strains showed *E. dispar*-type mobility (Tachibana *et al.* 2007; Takano *et al.* 2007; Suzuki *et al.* 2007). However, gene analyses have shown that there are fewer differences in the amino acid sequence of PGM between the *E. nuttalli* NASA6 and P19-061405 strains than between NASA6 and *E. histolytica* or P19-061405 and *E. dispar*.

Cultured trophozoites of the NASA6 strain were scored positive by the *E. histolytica* antigen detection kit, similar to the P19-061405 and EHMfas1 strains (Takano *et al.* 2005; Tachibana *et al.* 2007). However, none of the 30 fecal samples were found to be positive using this kit. Suzuki *et al.* (2007) have reported positive results in fecal samples analysed with this kit, but the samples were tested after a freezing-thawing procedure (personal communication). Therefore, the amount of antigen extracted may account for the different results. It is also possible that the anti-*E. histolytica* lectin antibody in the kit has low reactivity to *E. nuttalli* and comparative analysis of the antigen is required to address this issue.

Morphological differences of *E. nuttalli* compared with *E. histolytica* and *E. dispar* were not evident in cysts and xenically cultured trophozoites under light microscopy. However, trophozoites of *E. nuttalli*, as well as those of *E. histolytica*, were axenized easily in comparison with *E. dispar* (Clark, 1995; Kobayashi *et al.* 2005). The length range of living trophozoites of *E. nuttalli* in axenic culture overlaps with that of *E. histolytica*, but the *E. nuttalli* trophozoites tend to be elongated in comparison with *E. histolytica* trophozoites (Espinosa-Cantellano *et al.* 1998). The average diameters of chilled trophozoites of *E. nuttalli* NASA6 and P19-061405 strains adapted to axenic culture conditions were significantly smaller than that of *E. histolytica* HM-1:IMSS. *E. histolytica* trophozoites obtained from intestinal or liver lesions are generally larger than those found in cultures (Martínez-Palomo, 1993), but the *E. nuttalli* trophozoites observed in liver in this study seemed to be as small as those in culture. It is unclear whether the size difference influences the overall characteristics of *E. nuttalli*, but this difference has also been found in a comparison of *E. histolytica* and *E. histolytica*-like Laredo (*E. moshkovskii*) trophozoites (Diamond, 1968; López-Revilla and Gómez-Domínguez, 1988).

The liver damage produced in hamsters inoculated with *E. nuttalli* trophozoites was similar to that described in the same species challenged with *E. histolytica* trophozoites (Tsutsumi *et al.* 1984). This suggests similar physiopathological mechanisms of tissue damage, including an important role of lysed inflammatory cells (Perez-Tamayo *et al.* 1991; Tsutsumi and Shibayama, 2006). Ultrastructural analysis of the amoeba-inflammatory cell interaction has shown that *E. nuttalli* carries a similar virulent capacity to destroy target cells, including lysis of inflammatory cells and endocytosis, despite the smaller size of trophozoites of the *E. nuttalli* NASA6 strain compared to the *E. histolytica* HM-1:IMSS strain (Tsutsumi and Martínez-Palomo, 1988).

If *E. nuttalli* is able to infect humans, it may be of concern as a zoonotic hazard. Therefore, a stool examination was performed on the 4 keepers taking care of the monkeys in the park. No parasites were detected from samples by direct microscopy or in culture in Tanabe-Chiba medium (data not shown). It remains possible that *E. nuttalli* is infective in humans, but *Entamoeba* with the zymodeme pattern of *E. nuttalli* has not been detected in more than 2500 separate isolations characterized to date (Sargeaunt, 1988). However, the results in this study show that the *E. nuttalli* NASA6 strain isolated from Japanese macaque is potentially virulent, and we suggest that *E. nuttalli* should be recognized as a common parasite in macaques and should be discriminated from *E. histolytica* and *E. dispar* in routine analysis.

We thank M. Johshita (Nagasaki University) for her help with xenic culture. We also thank the staff in the Teaching and Research Support Center, Tokai University School of Medicine, for their help in DNA sequencing. This work was supported by a Grant-in Aid for Scientific Research from the Japanese Society for the Promotion of Science (to H.T.) and a Cooperative Research Grant 2006-18-C-4 from the Institute of Tropical Medicine, Nagasaki University (to H.K.).

REFERENCES

Castellani, A. (1908). Note on a liver abscess of amoebic origin in a monkey. *Parasitology* **1**, 101–102.

Chu, J. H., Lin, Y. S. and Wu, H. Y. (2007). Evolution and dispersal of three closely related macaque species, *Macaca mulatta*, *M. cyclopis*, and *M. fuscata*, in the eastern Asia. *Molecular Phylogenetics and Evolution* **43**, 418–429.

Clark, C. G. (1995). Axenic cultivation of *Entamoeba dispar* Brumpt 1925, *Entamoeba insolita* Geiman and Wichterman 1937 and *Entamoeba ranarum* Grassi 1879. *Journal of Eukaryotic Microbiology* **42**, 590–593.

Diamond, L. S. (1968). Techniques of axenic cultivation of *Entamoeba histolytica* Schaudinn, 1903

and *E. histolytica*-like amebae. *Journal of Parasitology* **54**, 1047–1056.

Diamond, L. S. and Clark, C. G. (1993). A redescription of *Entamoeba histolytica* Schaudinn, 1903 (Emended Walker, 1911) separating it from *Entamoeba dispar* Brumpt, 1925. *Journal of Eukaryotic Microbiology* **40**, 340–344.

Diamond, L. S., Harlow, D. R. and Cunnick, C. C. (1978). A new medium for the axenic cultivation of *Entamoeba histolytica* and other *Entamoeba*. *Transactions of the Royal Society of Tropical Medicine and Hygiene* **72**, 431–432.

Espinosa-Cantellano, M., Gonzáles-Robles, A., Chávez, B., Castañón, G., Argüello, C., Lázaro-Haller, A. and Martínez-Palomo, A. (1998). *Entamoeba dispar*: ultrastructure, surface properties and cytopathic effect. *Journal of Eukaryotic Microbiology* **45**, 265–272.

Ghosh, S., Frisardi, M., Ramirez-Avila, L., Descoteaux, S., Sturm-Ramirez, K., Newton-Sanchez, O. A., Santos-Preciado, J. I., Ganguly, C., Lohia, A., Reed, S. and Samuelson, J. (2000). Molecular epidemiology of *Entamoeba* spp.: evidence of a bottleneck (Demographic sweep) and transcontinental spread of diploid parasites. *Journal of Clinical Microbiology* **38**, 3815–3821.

Hayasaka, K., Fujii, K. and Horai, S. (1996). Molecular phylogeny of macaques: implications of nucleotide sequences from an 896-base pair region of mitochondrial DNA. *Molecular Biology and Evolution* **13**, 1044–1053.

Hegner, R. and Schumaker, E. (1928). Some intestinal amoebae and flagellates from the chimpanzee, three-toed sloth, sheep and guinea-pig. *Journal of Parasitology* **15**, 31–37.

Kobayashi, S., Imai, E., Haghighi, A., Khalifa, S. A., Tachibana, H. and Takeuchi, T. (2005). Axenic cultivation of *Entamoeba dispar* in newly designed yeast extract-iron-gluconic acid-dihydroxyacetone-serum medium. *Journal of Parasitology* **91**, 1–4.

López-Revilla, R. and Gómez-Domínguez, R. (1988). Trophozoite and nuclear size, DNA base composition, and nucleotide sequence homology of several *Entamoeba* strains in axenic culture. *Parasitology Research* **74**, 424–430.

Martínez-Palomo, A. (1993). Parasitic amebas of the intestinal tract. In *Parasitic Protozoa*, 2nd Edn., (ed. Kreier, J. P. and Baker, J. R.), Vol. 3, pp. 65–141. Academic Press, San Diego, USA.

McLean, I. W. and Nakane, P. K. (1974). Periodate-lysine-paraformaldehyde fixative. A new fixation for immunoelectron microscopy. *Journal of Histochemistry and Cytochemistry* **22**, 1077–1083.

Muriuki, S. M., Murugu, R. K., Munene, E., Karere, G. M. and Chai, D. C. (1998). Some gastro-intestinal parasites of zoonotic (public health) importance commonly observed in old world non-human primates in Kenya. *Acta Tropica* **71**, 73–82.

Neal, R. A. (1966). Experimental studies on *Entamoeba* with reference to speciation. *Advances in Parasitology* **4**, 1–51.

Perez-Tamayo, R., Martinez, R. D., Montfort, I., Becker, I., Tello, E. and Perez-Montfort, R. (1991). Pathogenesis of acute experimental amebic liver abscess in hamsters. *Journal of Parasitology* **77**, 982–988.

Rivera, W. L. and Kanbara, H. (1999). Detection of *Entamoeba dispar* DNA in macaque feces by polymerase chain reaction. *Parasitology Research* **85**, 493–495.

Robinson, G. L. (1968). The laboratory diagnosis of human parasitic amoebae. *Transactions of the Royal Society of Tropical Medicine and Hygiene* **62**, 285–294.

Sargeaunt, P. G. (1988). Zymodemes of *Entamoeba histolytica*. In *Amebiasis : Human Infection by* Entamoeba histolytica (ed. Ravdin, J. I.), pp. 370–387. John Wiley & Sons, New York, USA.

Smith, J. M. and Meerovitch, E. (1985). Primates as a source of *Entamoeba histolytica*, their zymodeme status and zoonotic potential. *Journal of Parasitology* **71**, 751–756.

Suzuki, J., Kobayashi, S., Murata, R., Yanagawa, Y. and Takeuchi, T. (2007). Profiles of a pathogenic *Entamoeba histolytica*-like variant with variations in the nucleotide sequence of the small subunit ribosomal RNA isolated from a primate (De Brazza's guenon). *Journal of Zoo and Wildlife Medicine* **38**, 471–474.

Tachibana, H., Cheng, X. J., Kobayashi, S., Fujita, Y. and Udono, T. (2000). *Entamoeba dispar*, but not *E. histolytica*, detected in a colony of chimpanzees in Japan. *Parasitology Research* **86**, 537–541.

Tachibana, H., Cheng, X. J., Kobayashi, S., Matsubayashi, N., Gotoh, S. and Matsubayashi, K. (2001). High prevalence of infection with *Entamoeba dispar*, but not *E. histolytica*, in captive macaques. *Parasitology Research* **87**, 14–17.

Tachibana, H., Yanagi, T., Pandey, K., Cheng, X. J., Kobayashi, S., Sherchand, J. B. and Kanbara, H. (2007). An *Entamoeba* sp. strain isolated from rhesus monkey is virulent but genetically different from *Entamoeba histolytica*. *Molecular and Biochemical Parasitology* **153**, 107–114.

Takano, J., Narita, T., Tachibana, H., Shimizu, T., Komatsubara, H., Terao, K. and Fujimoto, K. (2005). *Entamoeba histolytica* and *Entamoeba dispar* infections in cynomolgus monkeys imported into Japan for research. *Parasitology Research* **97**, 255–257.

Takano, J., Narita, T., Tachibana, H., Terao, K. and Fujimoto, K. (2007). Comparison of *Entamoeba histolytica* DNA isolated from a cynomolgus monkey with human isolates. *Parasitology Research* **101**, 539–546.

Takano, J., Tachibana, H., Kato, M., Narita, T., Yanagi, T., Yasutomi, Y. and Fujimoto, K. (2009). DNA characterization of simian *Entamoeba histolytica*-like strains to differentiate them from *Entamoeba histolytica*. *Parasitology Research* **105**, (in the Press). doi:10.1017/S00436-009-1480-3

Tsutsumi, V., Mena-Lopez, R., Anaya-Velazquez, F. and Martinez-Palomo, A. (1984). Cellular bases of experimental amebic liver abscess formation. *American Journal of Pathology* **117**, 81–91.

Tsutsumi, V. and Martínez-Palomo, A. (1988). Inflammatory reaction in experimental hepatic amebiasis. An ultrastructural study. *American Journal of Pathology* **130**, 112–119.

Tsutsumi, V. and Shibayama, M. (2006). Experimental amebiasis: a selected review of some in vivo models. *Archives of Medical Research* **37**, 210–220.

Verweij, J. J., Polderman, A. M. and Clark, C. G. (2001). Genetic variation among human isolates of uninucleated cyst-producing *Entamoeba* species. *Journal of Clinical Microbiology* **39**, 1644–1646.

Verweij, J. J., Vermeer, J., Brienen, E. A., Blotkamp, C., Laeijendecker, D., van Lieshout, L. and Polderman, A. M. (2003). *Entamoeba histolytica* infections in captive primates. *Parasitology Research* **90**, 100–103.

Wenyon, C. M. (1965). *Protozoology: A Manual for Medical Men, Veterinarians and Zoologists*. Hafner Publishing Company, New York, USA.

World Health Organization (1997). Amoebiasis. *Weekly Epidemiological Record* **72**, 97–99.

Parasitol Res (2009) 105:977–987
DOI 10.1007/s00436-009-1478-x

ORIGINAL PAPER

Involvement of serine proteases in the excystation and metacystic development of *Entamoeba invadens*

Asao Makioka · Masahiro Kumagai · Seiki Kobayashi · Tsutomu Takeuchi

Received: 13 March 2009 / Accepted: 8 May 2009 / Published online: 29 May 2009

Abstract Although the functions of cysteine proteases involved in the pathogenicity and differentiation of *Entamoeba histolytica* have been demonstrated, little is known about the functions of serine proteases. We examined the involvement of serine proteases in amoebic excystation and metacystic development using inhibitors specific for serine proteases. *Entamoeba invadens* IP-1 strain was used as the model of excystation and metacystic development of *E. histolytica*. Four serine protease inhibitors, phenylmethanesulfonyl fluoride (PMSF), 4-(2-aminoethyl) bezensulfonyl-fluoride hydrochloride, 3, 4-dichloroisocoumarin, and *N*-tosyl-phe-chloromethylketone, decreased the number of metacystic amoebae in a dose-dependent manner, without showing cytotoxicity to cysts. PMSF inhibited not only the increase but also the development of metacystic amoebae as determined by the change of nucleus number from four- to one-nucleate amoebae. The protease activity in cyst lysates was also inhibited by PMSF and the band of protease on gelatin sodium dodecyl sulfate polyacrylamide gel electrophoresis was weaker than controls when treated with PMSF. Three serine protease families, S28 (three types), S9 (two), and S26 (one) were retrieved from the database of *E. invadens*. Phylogenetic analysis revealed that amebic enzymes from the serine protease families formed different clades from those from other organisms. The expression levels of these serine proteases in cysts 5 h after the induction of excystation as assessed by real-time reverse transcriptase polymerase chain reaction (RT-PCR) were higher than those observed prior to induction assayed by real-time RT-PCR; the increase in one type of S9 (named S9-3) expression was the highest. The expression of S9 enzymes also increased from cysts to trophozoites higher than the other family serine proteases. Thus, the results show that *Entamoeba* uses their serine proteases in the excystation and metacystic development, which leads to successful infection.

A. Makioka (✉) · M. Kumagai
Department of Tropical Medicine,
Jikei University School of Medicine,
3-25-8 Nishi-shinbashi,
Minato-ku, Tokyo, 105-8461, Japan
e-mail: makioka@jikei.ac.jp

S. Kobayashi · T. Takeuchi
Department of Tropical Medicine and Parasitology,
School of Medicine, Keio University,
35 Shinanomachi,
Shinjuku-ku, Tokyo, 160-8582, Japan

Introduction

Excystation and metacystic development are important initial processes necessary for establishing *Entamoeba* infection. Their processes have morphologically been described for *Entamoeba histolytica* (Dobell 1928; Cleveland and Sanders 1930). Since *E. histolytica* does not encyst efficiently in axenic culture, *Entamoeba invadens*, a reptilian parasite, has been used as a useful model for the study of encystation and excystation (López-Romero and Villagómez-Castro 1993; Eichinger 1997). Excystation is the process by which the whole organism emerges outside through a minute perforation in the cyst wall. Metacystic development is the process by which a hatched metacystic amoeba with four nuclei divides to produce eight amoebulae, which grow to become trophozoites (Dobell 1928; Cleveland and Sanders 1930; Geiman and Ratcliffe 1936). The transfer of *E. invadens* cysts in the encystation medium to the growth medium induces in vitro excystation (McConnachie 1955;

Rengpien and Bailey 1975; Garcia-Zapien et al. 1995; Makioka et al. 2002).

We first focused on proteases and evaluated their roles in the excystation, since perforation of the cyst wall, which is composed of chitin and proteins, is necessary for the excystation. Among the proteases, cysteine proteases have been relating to the differentiation and pathogenicity of many protozoan parasites including *E. histolytica* (McKerrow 1989; Rosenthal 1999; Que and Reed 2000; Sajid and McKerrow 2002). We also demonstrated the involvement of cysteine proteases in the excystation and metacystic development of *E. invadens* (Makioka et al. 2005).

Serine proteases are also one of the main classes of proteases and carry out a diverse array of physiological functions (Yousef et al. 2003). However, little is known about their functions in *Entamoeba*. Although the involvement of serine proteases in the encystation of *E. invadens* was demonstrated using 4-(2-aminoethyl) bezensulfonyl-fluoride hydrochloride (AEBSF), an inhibitor (Riahi and Ankri 2000), their roles in the excystation and metacystic development of *Entamoeba* have not so far been reported. In this study, we showed that the excystation and metacystic development of *E. invadens* were inhibited by serine protease inhibitors and that expression of serine protease mRNA highly increased following the induction of excystation.

Materials and methods

Serine protease inhibitors

Four serine protease inhibitors, phenylmethanesulfonyl fluoride (PMSF), AEBSF, 3, 4-dichloroisocoumarin (DCI), and *N*-tosyl-phe-chloromethylketone (TPCK) were used in this study and they were purchased from Calbiochem (San Diego, CA, USA). All of the inhibitors were dissolved in dimethyl sulfoxide (DMSO). The control cultures received the same volume of DMSO.

Culture, encystation, and excystation of *E. invadens*

Trophozoites of the IP-1 strain of *E. invadens* were cultured in an axenic growth medium, BI-S-33 (Diamond et al. 1978), at 26°C. To obtain cysts, trophozoites (5×10^5cells/ml) were transferred to an encystation medium called 47% LG (LG is BI without glucose; Sanchez et al. 1994). After 3 days of incubation, the percentage of encystation reached 80% on average. The cells were harvested and treated with 0.05% sarkosyl (Sigma Chemical Co., St. Louis, MO, USA) to destroy the trophozoites (Sanchez et al. 1994). The remaining cysts were washed with phosphate-buffered saline, counted, and then suspended in the growth medium. The viability of the cysts was determined by Trypan blue dye exclusion, and the number of nuclei per cyst was determined after staining in suspension with modified Kohn's staining (Kumagai et al. 2001). Cyst preparation included 30% dead or denatured cysts and 70% viable cysts, where four-nucleate cysts are 30% and one- to three-nucleate cysts are 70%.

For the experiments on the excystation and metacystic development of *E. invadens*, duplicate cultures of 5×10^5 cysts/ml were incubated with inhibitors for 3 days. Metacystic amoebae were counted in a hemocytometer on days 1 and 3, and their viability was determined by Trypan blue dye exclusion. Metacystic development was determined by the number of nuclei per amoeba, which decreases from four to one with the development. The cells were cultured for 1 or 3 days with or without inhibitor and stained with modified Kohn. The number of nuclei per amoeba was determined by the double counting of at least 100 amoebae. Viable metacystic amoebae and cysts were clearly distinguished as light yellow and light blue in color, respectively. The former one was also identified by positive motility.

Assay of serine protease activity

For the assay of serine protease activity, cysts (2×10^7/ml) were harvested, washed, and subjected to three freeze–thaw cycles in a phosphate-buffered saline. After centrifugation, the supernatants were obtained as lysates. The activity was quantified by the cleavage of the fluorogenic synthetic substrate *N*-succinyl-L-Ala-L-Ara-L-Phe-7-amino-4-methylcoumarin (Suc-AAF-AMC; Sigma) as previously described (Barrios-Ceballos et al. 2005). Briefly, 15 µl of sample was added to 185 µl of reaction buffer (50 mM Tris-HCl, pH8.0, 10 mM NaCl, and 50 mM $CaCl_2$) with 0.05 mM substrate and incubated for 15 min at 37°C. The reactions were stopped by adding 2.8 ml of 0.1 M glycine, pH10.0, and fluorescence was read at 380 nm excitation and 460 nm emission in a fluorometer Picofluor (Turner Biosystems, Sunnyvale, CA, USA). To determine the inhibition of the amoebic enzyme by PMSF, the lysates were preincubated for 15 min at room temperature with 0.5 and 1 mM of PMSF before adding it to the reaction buffer.

Gelatin substrate gel electrophoresis

Protease activity in cyst lysates was assessed by gelatin substrate gel electrophoresis as previously described (Keene et al. 1986). The cysts were solubilized using a Laemmli sample buffer (Laemmli 1970) without a reducing agent. After centrifugation, the supernatants were treated with the

Table 1 Sequence of primers used for real-time RT-PCR

Genes	Forward primers	Reverse primers
EiS28-1	TGGCGACCAACCAATTTACA	TCTTATAGAGTTGTTCGATATTGGCATT
EiS28-2	AACGTCGCGTTCACAAAT	GTCCACTGCGTCTTGTTGAGTAA
EiS28-3	CGATTTTGGTGAGGATGACATTC	GCCCGCCAAAGCTGTTC
EiS9-2	TTCCAGTTCTTCCTCCTTTTCCT	CAACCGGCGAAGTCTAACAAG
EiS9-3	CGTCCCACCACGTCTTCAA	TCGGTTGTCGGGACATAAGC
EiS26	GCGCCATTACAACAAATGATGT	CCAAACTGAAACGCATTCTGAA
EirRNA	GTGACGCGCATGAATGGA	TTCCCTTGACTGTGGTTTCACTAG

Laemmli sample buffer. Sodium dodecyl sulfate polyacrylamide gel electrophoresis (SDS-PAGE) was conducted in nonreducing conditions on 10% gels that had been copolymerized with 0.1% gelatin. The cyst lysates, equivalent to 5×10^4 cysts, were loaded per lane and electrophoresed. The gels was washed for 1 h in 2.5% Triton X-100 to remove SDS, rinsed twice in distilled water, and incubated in 50 mM Tris-HCl (pH8.0) buffer containing 50 mM $CaCl_2$ and 0.15 mM Suc-AAF-AMC with or without 1 mM PMSF for 12–18 h at 37°C. After staining with Coomassie blue and several cycles of destaining, the protease activity was detected as clear bands on the Coomassie blue-stained background of the control gels.

Identification of *E. histolytica* and *E. invadens* serine protease genes

The amino acid sequences of proteins from *E. histolytica* and *E. invadens* predicted at the J. Craig Venter Institute (JCVI; formerly The Institute for Genomic Research; http://www.jcvi.org/) were screened out if they had peptidase domains using the Pfam database (http://pfam.sanger.ac.uk/) and selected depending on their expectation (*e*) values (lower *e* values mean higher reliability of the selection). The selected genes and their predicted amino acid sequences were further checked individually for their sequences, domains, and similarity to serine protease sequences from other organisms against the database available at JCVI and the National Center for Biotechnology Information (NCBI; http://www.ncbi.nih.gov/) using the blastn, blastp, and tbastn algorithms.

Preparation of RNA and cDNA

RNA was isolated from cysts and trophozoites of *E. invadens* by Sepazol RNA I (Nacalai Tesque, Kyoto, Japan) containing phenol, ammonium thiocyanate, and 8-quinolinol according to the manufacturer's instructions. The total RNA isolated was first treated with DNase I (Invitrogen, Carlsbad, CA, USA) and then transcribed to cDNA using SuperScript III (Invitrogen).

Cloning and sequencing of *E. invadens* serine protease genes

A protein-coding region of *E. invadens* serine protease genes flanked by additional *Bam*HI and *Hind* III sites for EiS28-1, EiS28-2, EiS28-3, EiS9-3, or *BamH*I and *Sph* I sites for EiS9-2 was amplified by polymerase chain reaction (PCR) using cDNA as a template and the following sense and antisense primers: 5′-TTT*GGATCC*CATGCAGATCTTTTTC-3′ and 5′-AGCT*AAGCTT*TTAATATCTTTTGATAAGTTC-3′ (EiS28-1), 5′-TTT*GGATCC*CATGATTCTGTTCTTTC-3′ and 5′-AGCT*AAGCTT*TTACTTCTTGGGG-3′(EiS28-2), 5′-TTT*GGATCC*ATGCTTCTGCTG-3′ and 5′-AGCT*AAGCTT*TTATTCCTTCTTTGGC-3′ (EiS28-3), 5′-AAA*GGATCC*CATGTTCCAGTTCTTC-3′ and 5′-AACAT*GCATGC*TTATGCTTGGAGGTA-3′ (EiS9-2), 5′-TTT*GGATCC*CATGCTCCTGC-3′ and 5′-ACAT*AAGCTT*TCACTTCAATTGCTCG-3′ (EiS9-3), and 5′-TTT*GGATCC*CATGCTTGCGC-3′ and 5′-AGCT*AAGCTT*TCACTGATCTTTGTTAAG-3′ (EiS26), where the restriction sites are italicized. The cycling parameters of PCR were (1) denaturation at 94°C for 30 s, (2) annealing at 55°C for 30 s, (3) elongation at 72°C for 1 min, (4) 30 cycles. PCR products were electrophoresed, purified with Geneclean II Kit (BIO 101, Vista, CA, USA), cloned into *Bam*HI and *Hind*III- or *BamH*I and *Sph*I-digested pQE31 (Qiagen, Hilden, Germany), and sequenced. The nucleotide sequences of *E. invadens* serine proteases reported in this paper are available in the DNA Data Bank of Japan (DDBJ) database under the accession numbers in Table 1. The nucleotide sequence of real-time reverse transcriptase (RT) product for *E. invadens* rRNA is available under the accession number of AB481113.

Phylogenetic analyses

The amino acid sequences of the serine protease families, S28, S9, and S26 from organisms including *E. histolytica*, *Entamoeba dispar*, and *E. invadens*, were retrieved from

the databases available at JCVI and NCBI. In Kyoto Encyclopedia of Genes and Genomes (KEGG; http://www.genome.ad.jp/kegg/; Kanehisa and Goto 2000), the lysosomal Pro-X carboxypeptidase (PRCP) [EC 3.4.16.2], dipeptidyl-peptidase 7 [EC 3.4.14.2], and protease, serine, 16 (thymus) [PRSS16; EC 3.4.-.-] are classified in family S28; prolyl endopeptidase (PREP) [EC 3.4.21.26], dipeptidyl aminopeptidase (STE13) [EC 3.4.14.-], dipeptidyl-peptidase 4 (DPP4) [EC 3.4.14.5], DPP8 [EC 3.4.14.5], DPP9 [EC 3.4.14.5], acylaminoacyl-peptidase (APEH) [EC 3.4.19.1], fibroblast activation protein, alpha (FAP) [EC 3.4.21.-], and oligopeptidase B (ptrB) [EC 3.4.21.83] are in family S9; signal peptidase I [EC 3.4.21.89] and mitochondrial inner membrane protease subunit 1 (IMP1) and IMP2 [EC 3.4.99.-] are in family S26. The phylogenetic analyses were performed with CLUSTAL W (Thompson et al. 1994) version 1.83 using the neighbor-joining (NJ) method (Saitou and Nei 1987). Unrooted NJ trees were drawn with TreeView (Page 1996) version 1.6.6. Branch lengths and bootstrap values (1,000 replicates; Felsenstein 1985) were derived from the NJ analysis.

Real-time RT-PCR

Real-time reverse transcriptase-polymerase chain reaction was used to quantify serine protease mRNAs of *E. invadens*. This was carried out using an ABI real-time PCR system 7300 (Applied Biosystems, Foster City, CA, USA) with Power SYBR Green PCR Master Mix. Primers were designed by ABI Primer Express software. The reaction mix contained 200 nmol primers (see Table 2), 10 μl SYBR green mix, and template cDNA in a volume of 20 μl in RNase-free water. The "comparative Ct" method (outlined in ABI Prism 7700 Sequence Detection System Bulletin #2) was used to determine the relative quantities of the mRNA expression level of cysts before and 5 h after the induction of excystation and trophozoites. Ribosomal RNA was used as the endogenous control. A validation curve using serial dilutions of cDNA was used to ensure that the replication efficiencies of the tested genes. After initial denaturation for 10 min at 95°C, the amplification cycle (repeated 40 times) was as follows: 15 s at 95°C and 1 min at 60°C. The relative mRNA levels were expressed against those of cysts as 1.

Results

Effect of serine protease inhibitors on the number of metacystic amoebae of *E. invadens*

The effect of serine protease inhibitors on the number of metacystic amoebae of *E. invadens* after the transfer of cysts to a growth medium is shown in Fig. 1. All inhibitors tested were effective. The number of metacystic amoebae in cultures with 0.1 mM PMSF was comparable to the controls, whereas it significantly decreased in cultures with 0.5 and 1 mM PMSF compared to the controls. Similarly, metacystic amoebae decreased in number during incubation in cultures with 0.5 and 1 mM AEBSF. Ten-micromolar DCI significantly decreased the number of metacystic amoebae and more than 50 μM TPCK had the same effect.

The effects of serine protease inhibitors on cyst viability are shown in Fig. 2. The number of viable cysts in the control cultures decreased during incubation. It is considered that most immature cysts contained in culture

Table 2 Identification of serine protease genes in *E. histolytica* and *E. invadens* genome databases

Name	Name in Tillack et al. (2007)	Accession no.		*e* value
E. histolytica				
EhS28-1	EhSP28-3	XM_646997	Peptidase_S28	9.3e−106
EhS28-2	EhSP28-2	XM_643899	Peptidase_S28	1.7e−90
EhS28-3	EhSP28-1	XM_6516702	Peptidase_S28	1.7e−86
EhS9-1	EhSP9-3	XM_6512882	Peptidase_S9	6.7e−57
EhS9-2	EhSP9-2	XM_650130	Peptidase_S9	1.7e−56
EhS9-3	EhSP9-4-2	XM_643321	Peptidase_S9	1.4e−06
EhS26	EhSP26-1	XM_648050	Peptidase_S24	6.9e−06
E. invadens				
EiS28-1		AB474585	Peptidase_S28	2.4e−100
EiS28-2		AB474586	Peptidase_S28	4.6e−100
EiS28-3		AB480531	Peptidase_S28	8.1e−86
EiS9-2		AB474587	Peptidase_S9	7.1e−54
EiS9-3		AB480532	Peptidase_S9	5.3e−08
EiS26		AB480533	Peptidase_S24	1.5e−07

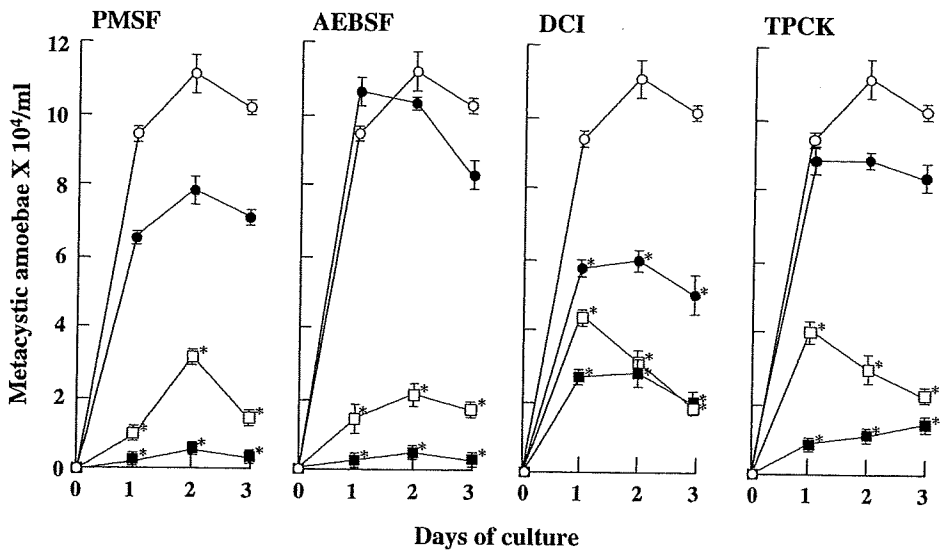

Fig. 1 Effect of serine protease inhibitors on the number of metacystic amoebae of *E. invadens*. Cysts were transferred to a growth medium containing various concentrations of cysteine protease inhibitors PMSF, AEBSF, TPCK, and DCI. The mean numbers ± standard errors of metacystic amoebae for the duplicate cultures are plotted (each *asterisk* indicates $P<0.05$). Concentrations of 0, 0.1, 0.5, and 1 mM for PMSF and AEBSF and 0, 10, 50, and 100 μM for DCI and TPCK are indicated by the *white circles*, *black circles*, *white squares*, and *black squares*, respectively

degenerate or die during incubation. The number of viable cysts in cultures containing PMSF, AEBSF, DCI, or TPCK at all concentrations during incubation was comparable to that of the controls.

Effect of serine protease inhibitor on the metacystic development of *E. invadens*

The effect of serine protease inhibitor PMSF on metacystic development was examined by counting the number of nuclei per cell. As shown in Fig. 3, 5% of the metacystic amoebae were four nucleates on day1 of incubation in the control culture, whereas 33% of the amoebae were in culture with PMSF. The percentage of four-nucleate amoebae in the control culture was almost unchanged to 3% on day3, while the percentage of four-nucleate amoebae in culture with PMSF was still 26% on day3. Also, the percentage of one-nucleate amoebae in the control culture increased from 52% on day1 to 74% on day3, while the increase in culture with PMSF was from 15% on day1 to 32% on day3, suggesting the inhibition of metacystic development due to PMSF.

Inhibition of serine protease activity in cyst lysates by PMSF

We examined the effect of PMSF on serine protease activity in cyst lysates. As shown in Fig. 4, serine protease activity in cyst lysates against synthetic peptide substrate was inhibited by PMSF in a concentration-dependent manner. Gelatin substrate SDS-PAGE of cysts indicated a protease activity of a 56-kDa major band and broad bands of higher

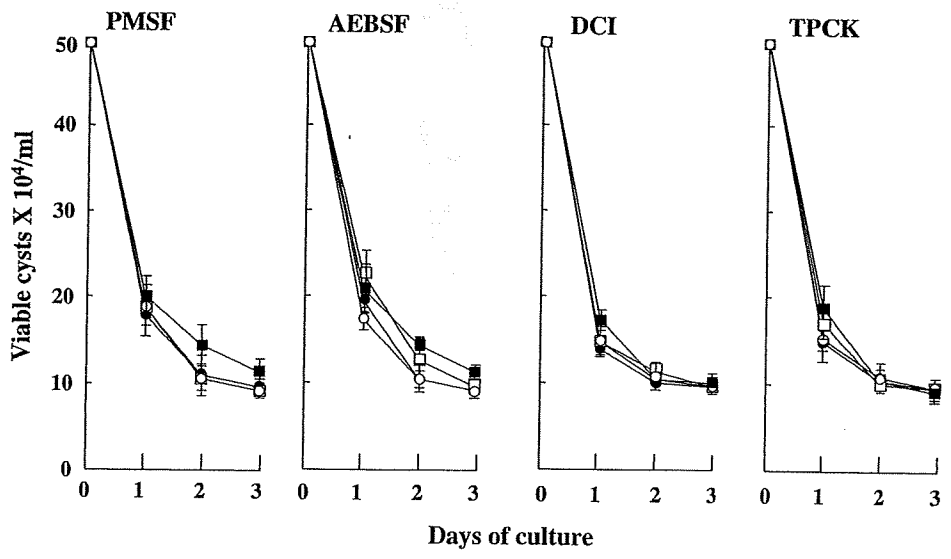

Fig. 2 Effect of serine protease inhibitors on the cyst viability of *E. invadens* in the growth medium. The experimental conditions were the same as those for Fig. 2. The mean numbers ± standard errors of viable cysts for the duplicate cultures are plotted. Concentrations are indicated in a similar manner as for Fig. 2

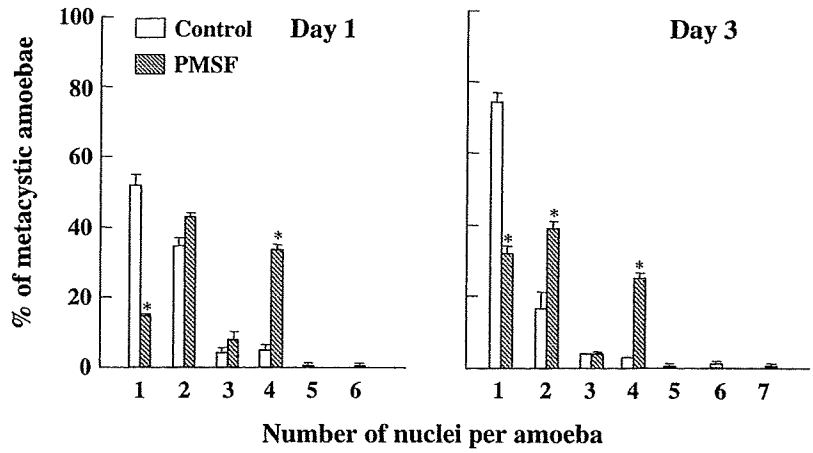

Fig. 3 The effect of PMSF on the metacystic development of *E. invadens*. The cysts were transferred to a growth medium with or without 0.5 mM of PMSF. The numbers of nuclei per metacystic amoeba stained with modified Kohn on days 1 and 3 of incubation were counted, and the percentage of amoebae in each class (*1–7* nucleate) was determined (each *asterisk* indicates $P<0.05$)

molecular weights. Most of these bands decreased in intensity in the presence of PMSF (Fig. 4).

Identification of serine protease genes in genome databases of *E. histolytica* and *E. invadens*

Search of genes of *E. histolytica* and *E. invadens* predicted at JCVI against Pfam database revealed seven and six serine protease genes of the S28, S9, and S24 family, respectively, which had significantly lower *e* values of less than 6.9e−06 for *E. histolytica* and 1.5e−07 for *E. invadens* (Table 1). The S24 and S26 family of serine proteases are shown separately in KEGG, but they are not in Pfam where the S26 is also shown as the S24. Therefore, we further confirmed *Entamoeba* S24 enzymes by homology search and identified those as the S26 enzyme. Thus, *E. histolytica* and *E. invadens* serine proteases were named in order of the *e* values and by their homology (Table 1).

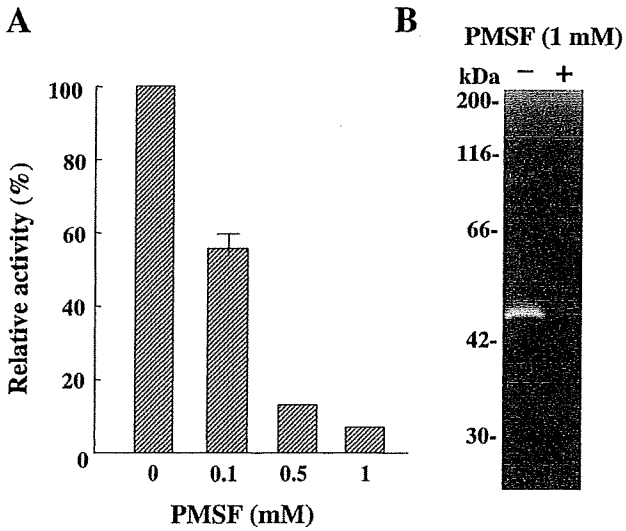

Fig. 4 The effect of PMSF on serine protease activity in the lysates of *E. invadens* cysts. **a** The lysates of *E. invadens* cysts (2×10^7/ml) were incubated with 0.1, 0.5, or 1 mM of PMSF. The percentages ± standard errors of activity against the control are plotted. **b** Gelatin substrate SDS-PAGE of the lysates of *E. invadens* cysts. Following the removal of SDS, the gels were incubated in buffer alone or with 1 mM PMSF

Phylogenetic analysis of serine proteases

Phylogenetic trees of the families S28, S9, and S26 of serine proteases from *Entamoeba* and other organisms were constructed (Figs. 5, 6, and 7). *Entamoeba* serine proteases of the family S28 belonged to PRSS16 [EC:3.4.-.-] formed a clade separated from those of other organisms including mammals, and EiS28-1, EiS28-2, and EiS28-3 were somewhat divergent from those of *E. histolytica* and *E. dispar* within the clade (Fig. 5). The family S9 of *Entamoeba* also formed a clade independent from those of all the other organisms, and EhS9-1, the homolog of which was not yet identified in *E. dispar* and *E. invadens*, was divergent from other S9 (S9-2 and S9-3) of *Entamoeba* (Fig. 6). As for the family S26 of serine proteases, all *Entamoeba* enzymes of this family belonged to signal peptidase I but not to IMP type. Signal peptidases of *Entamoeba* were also divergent from those of other organisms (Fig. 7).

Change in the expression level of serine proteases following the induction of excystation

In order to determine whether the mRNA levels of serine proteases are changed following the induction of excystation, mRNA levels of serine proteases in cysts were compared between before induction and 5 h after the induction of excystation by real-time RT-PCR using the primers shown in Table 2. As shown in Fig. 8, mRNA levels of all the family members in cysts 5 h after induction

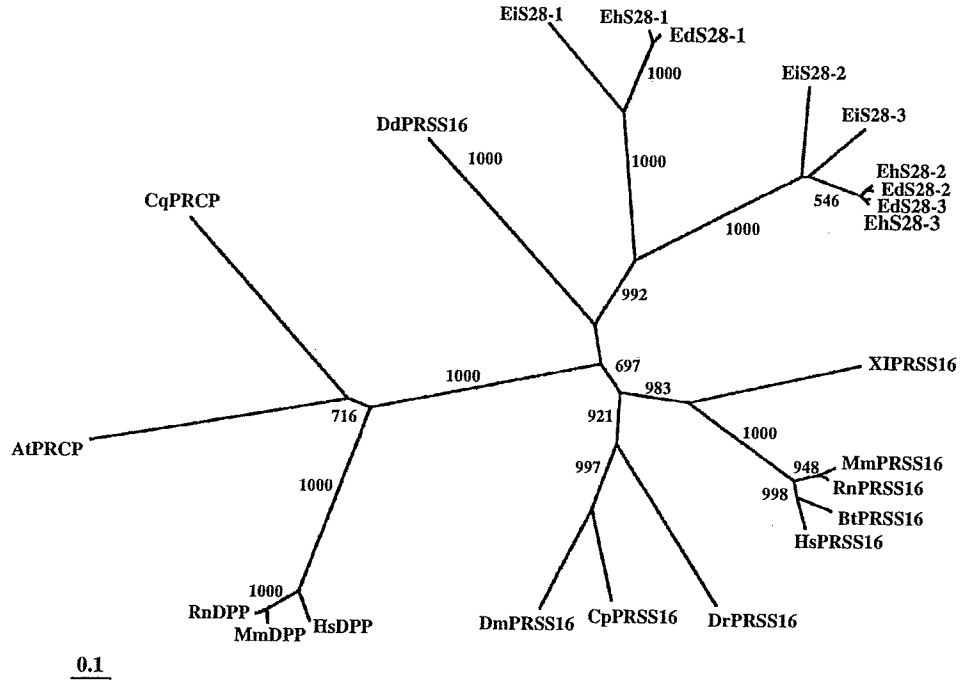

Fig. 5 Phylogenetic tree of S28 family of serine proteases. The tree was constructed by neighbor-joining distance analysis using the CLUSTAL W and TreeView programs. *Line lengths* indicate distances between nodes. The *bar* represents a distance of 0.1 amino acid changes per site. Bootstrap values for 1,000 replicates are shown at nodes. Abbreviations and accession numbers are Eh (*Entamoeba histolytica*) S28-1 (DDBJ/EMBL/GeneBank™ number, XP_652089), EhS28-2 (XP_64991), EhS28-3 (XP_656762); Ed (*E. dispar*) S28-1 (XP_001736631), EdS28-2 (XP_001733641), EdS28-3 (XP_001739195); Ei (*E. invadens*) S28-1 (AB474585), EiS28-2 (AB474586), EiS28-3 (AB480531); At (*Arabidopsis thaliana*) PRSS16 (NP_567999), AtPRCP (BAB10683); XI (*Xenopus laevis*) PRSS16 (AAI08760); Dd (*Dictylostelium discoidem*) PRSS16 (XP_644128); Cp (*Culex pipiens*) PRSS16 (EDS29541); Cq (*Culex quinquefasciatus*) PRCP (EDS38890); Dm (*Drosophila melanogaster*) PRSS16 (NP_648067); Dr (*Danio rerio*) PRSS16 (AAI29321); Mm (*Mus musculus*) PRSS16 (NP_062302), MmDPP (Q9ET22); Rn (*Rattus norvegicus*) PRSS16 (Q9EPB1), RnDPP (Q9EPB1); Bt (*Bos taurus*) PRSS16 (NP_001069798); Hs (*Homo sapiens*) PRSS16 (Q9NQE7), HsPRCP (NP_005031), HsDPP (Q9UHL4). *PRSS16* protease, serine, 16, *PRCP* lysosomal pro-X carboxypeptidase, *DPP* dipeptidyl-peptidase II

were significantly higher than those in cysts before induction, the highest being S9-3 enzyme among them.

Comparison of the expression level of serine proteases between cysts and trophozoites

The mRNA levels of serine proteases were compared between in cysts and trophozoites by real-time RT-PCR. As shown in Fig. 9, members (S9-2 and S9-3) of the S9 family had significantly higher levels in trophozoites than other family members, suggesting that they play important roles in trophozoites.

Discussion

The results of the present study strongly suggest the participation of serine proteases in the excystation and metacystic development of *E. invadens*. As cyst viability was not affected by the four serine protease inhibitors used, reduced excystation cannot be due to their toxic effect on cysts. The process of excystation includes the loosening and separation of amoeba from the cyst wall; the amoeba begins to move about within the cyst. The amoeba then flows back and forth through a small pore in the cyst wall and escapes from the cyst. Thus, cyst wall destruction is necessary for minute perforation of the cyst wall, which contains a mix of chitin and protein (Arroyo-Begovich and Carbez-Trejo 1982; Frisardi et al. 2000). Therefore, both chitinase and protease are essential for cyst wall destruction in the excystation process.

The cyst wall of *E. invadens* is a single and continuous fibrillar layer closely associated to the plasma membrane when observed by electron microscopy (Frisardi et al. 2000; Chávez-Munguía et al. 2003, 2007). An ultrastructural study demonstrated the presence of dense granules in the cytoplasm at the beginning of the excystation process and their increase during excystation (Chávez-Munguía et al. 2003, 2007). Many dense granules were frequently associated to the inner leaflet of the plasma membrane, and their liberation was suggested by the formation of thin finger-like projections of the plasma membrane, which held them

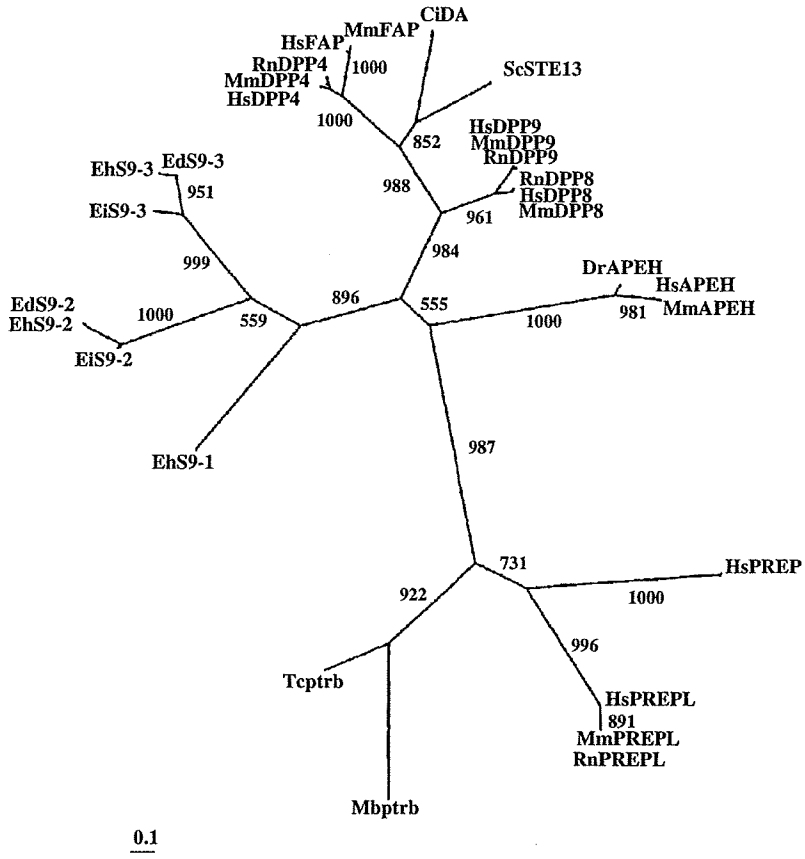

Fig. 6 Phylogenetic tree of S9 family of serine proteases. The tree was constructed and analyzed in a similar manner as for S28. Abbreviations except in Fig. 7 are EhS9-1 (XP_656380), EhS9-2 (XP_655222), EhS9-3 (XP_648413); EdS9-2 (XP_001740099), EdS9-3 (XP_001734149); EiS9-2 (AB474587), EiS9-3 (AB480532); Tc (*Trypanosoma cruzi*) ptrB (XP_806337); Mb (*Mycobacterium bovis*) ptrB (NP_854462); Ci (*Coccidioides immitis*) DA (XP_001248569); Sc (*Saccharomyces cerevisiae*) STE13 (CAA63182); DrAPEH (NP_942570); MmPREP (NP_035286), MmPREPL (NP_666096), MmDPP4 (NP_034204), MmDPP8 (NP_083182), MmDPP9 (NP_766212), MmAPEH (NP_666338), MmFAP (NP_032012); RnPREPL (NP_001010951), RnDPP4 (NP_036921), RnDPP8 (XP_236345), RnDPP9 (XP_217309); HsPREP (NP_002717), HsPREPL (NP_006027), HsDPP4 (NP_001926), HsDPP8 (NP_060213), HsDPP9 (NP_631898), HsAPEH (NP_001631), HsFAP (NP_004451). *ptrB* oligopeptidase B, *STE13* dipeptidyl aminopeptidase, *APEH* acylaminoacyl-peptidase, *PREP* prolyl oligopeptidase, *PREPL* prolyl oligopeptidase-like, *DA* dipeptidyl-aminopeptidase, *DPP* dipeptidyl-peptidase, *FAP* fibroblast activation protein, alpha

toward the fibrillar cyst walled space, suggesting participation in the excystation process (Chávez-Munguía et al. 2003, 2007). Since it was previously reported that proteolytic activity was related to dense granules of *E. histolytica* (León et al. 1997), it is possible that dense granules with proteases including serine proteases are liberated from the plasma membrane to the space for destruction of the cyst wall.

The excysted four-nucleate metacystic amoebae grow rapidly and divide to form eight amoebulae. The results indicate that serine proteases are also involved in this metacystic development because the percentage of four-nucleate amoebae was higher than in the controls on day3 of incubation. In this relation, our previous study demonstrated the inhibition of metacystic development by cysteine protease inhibitors (Makioka et al. 2005), suggesting the involvement of both proteases in the process.

Recently, ten serine proteases belonging to three different families have been identified in *E. histolytica* by homology search within the published amoeba genome (Tillack et al. 2007). EhS28-1, EhS28-2, EhS28-3, EhS9-1, EhS9-2, EhS9-3, and EhS26 in the present study (Table 2) corresponded to EhSP28-3, EhSP28-2, EhSP28-1, EhSP9-3, EhSP9-2, EhSP9-4-2 (XP_648413), and EhSP26-1 in the previous report (Tillack et al. 2007), respectively. EhSP9-1 and EhSP9-4- (XP_649111 and XP_655473) shown in the previous study (Tillack et al. 2007) have already been removed at JCVI. EhSP9-5 and EhSP26-2 (Tillack et al. 2007) were not shown in this study because of their higher *e* values in Pfam. Similarly, we identified six serine proteases of *E. invadens* belonging to S28, S9, and S26 families. Homolog of EhS9-1 was absent in *E. invadens* as well as *E. dispar*, suggesting that there are different

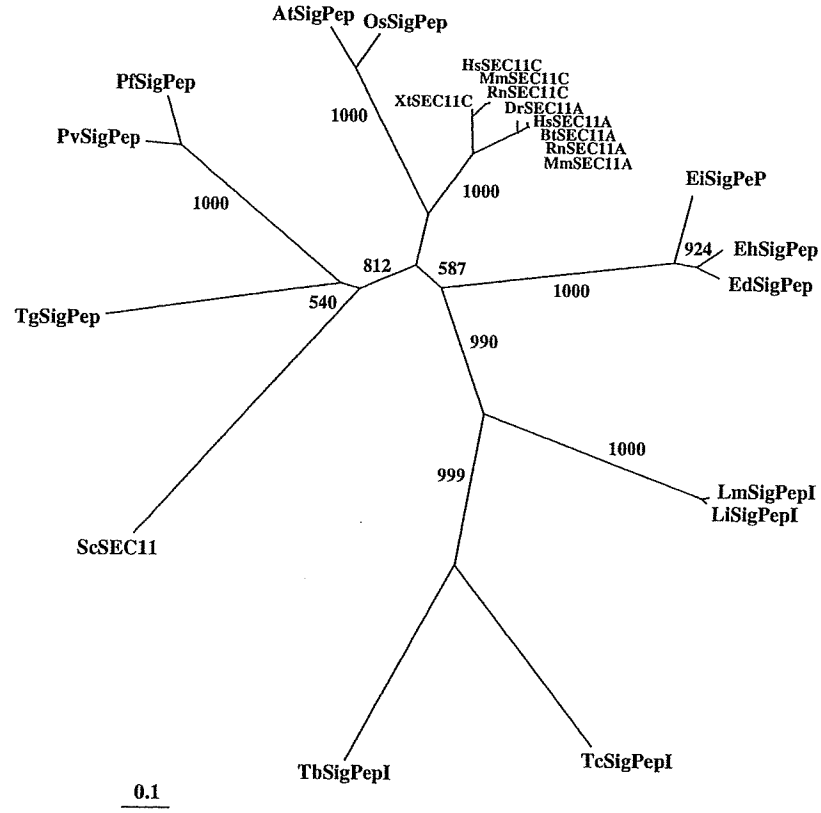

Fig. 7 Phylogenetic tree of S26 family of serine proteases. The tree was constructed and analyzed in a similar manner as for S28. Abbreviations except in Figs. 7 and 8 are EhSigPep (signal peptidase) (XP_653142), EdSigPep (XP_001740326), EiSigPep (AB480533), TcSigPepI (XP_814268), Tb (*T. brucei*) SigPepI (XP_844994), Lm (*Leishmania major*) SigPepI (XP_001681074), Li (*Leishmania infantum*) SigPepI (XP_001463385), Tg (*Toxoplasma gondii*) SigPep (EEB04328), Pv (*Plasmodium vivax*) SigPep (XP_00161410), Pf (*Plasmodium falciparum*) SigPep (XP_001350045), .AtSigPep (NP_175669), Os (*Oryza sativa*) SigPep (NP_001057371), Xt (*Xenopus tropicalis*) SEC11C (NP_001005129), ScSEC11C (P15367), DrSEC11A (NP_001002521), MmSEC11A (NP_064335), MmSEC11C (Q9D8V7), RnSEC11A (NP_113911), RnSEC11C (Q9WTR7), BtSEC11A (NP_776890), HsSEC11A (NP_055115), HsSEC11C (NP_150596). SEC11A and SEC11C belong to SigPepI

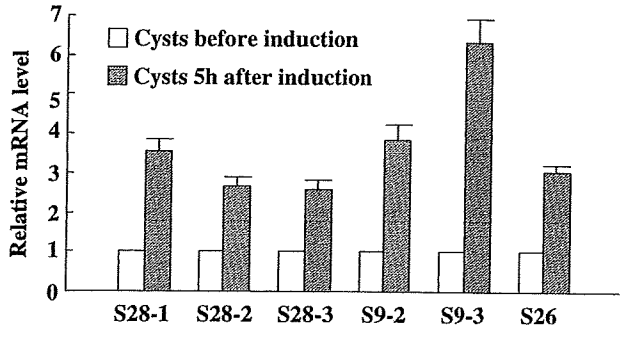

Fig. 8 Change in mRNA levels of serine proteases following the induction of excystation. The mRNA levels of five serine proteases before and 5 h after the induction of excystation were compared by real-time RT-PCR. The means ± standard errors of mRNA levels were shown relative to that of cysts as 1

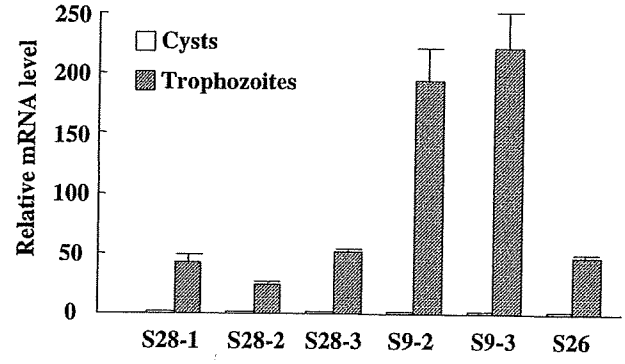

Fig. 9 Comparison of mRNA levels of serine proteases between cysts and trophozoites. The mRNA levels of five serine proteases between cysts and trophozoites were compared by real-time RT-PCR. The means ± standard error of mRNA levels were shown relative to those of cysts as 1

members within the same family of serine proteases due to species difference of *Entamoeba*.

The members of serine proteases identified in *E. histolytica* in this study was almost the same as those in the previous study (Tillack et al. 2007). Thus, there are much fewer serine proteases in *Entamoeba* than cysteine proteases, of which there are at least 50 (Bruchhaus et al. 2003). We also identified members of *E. invadens* and found only a slight difference between them by homology search. Since the homolog of EhS9-1 was absent in both *E. invadens* and nonpathogenic *E. dispar*, this enzyme is considered to be unique to *E. histolytica*. It remains unresolved whether the EhS9-1 is related to pathogenicity, like cysteine protease 5, whose gene is missing in *E. dispar* and was suggested to play a potential role in the host tissue destruction of *E. histolytica* (Bruchhaus et al. 2003). Since perforation of the cyst wall is necessary for excystation by all these *Entamoeba*, it is reasonable to consider that homologs of serine proteases of each species contribute to it.

The S28 family of serine proteases includes three members as shown at KEGG. Phylogenetic analysis revealed that S28 family members of *Entamoeba* belonged to members of the PRSS16 and formed an independent clade separate from those of other organisms, suggesting a difference in the primary structure between them. Since members of *Entamoeba* S28-1 and other S28-2, 3 formed a divergent clade, a difference in the primary structure between them is also suggested. Although the S9 family of serine proteases, called the prolyl oligopeptidase family, includes eight different members as shown at KEGG, those of *Entamoeba* did not form the same clade of any members from other organisms. This suggests that *Entamoeba* family S9 members are unique prolyl oligopeptidases. The S26 family members of *Entamoeba* belonging to signal peptidases also formed an independent clade from those of other organisms, suggesting their unique amino acid sequences.

The results indicate an increase in the expression level in cysts of all serine proteases belonging to different families following induction of excystation, suggesting the contribution of all these serine proteases to the excystation. Since EiS9-3 had the highest increase in the expression among them, it appears that it may be closely involved in the excystation.

The results of comparison of the expression of serine proteases between cysts and trophozoites demonstrated a difference in the expression level between members of the S9 and other families, where the S9 family members showing higher expression than other family members. In this relation, it was reported that S9-2 was highly expressed in trophozoites of *E. histolytica* but S28 members showed low or little expression (Tillack et al. 2007). Therefore, it is likely that the S9 members play a more important role than S28 members in trophozoites.

Further study is planned to evaluate the roles of serine proteases in the excystation by RNA interference and also to characterize their biochemical properties, which will lead to more accurate understanding of the process and also to the determination of targets for vaccination and chemotherapy to inhibit *Entamoeba* infection.

Acknowledgments We thank N. Watanabe and J. Watanabe for their valuable discussions with us, L. S. Diamond for supplying the *E. invadens*, K. Hiranuka and T. Katayama for their search of databases, and T. Yamashita and T. Tadano for their technical assistance. This work was supported in part by a Grant-in-Aid for Scientific Research from the Ministry of Education, Culture, Sports and Technology of Japan.

References

Arroyo-Begovich A, Carbez-Trejo A (1982) Location of chitin in the cyst wall of *Entamoeba invadens* with the colloidal gold tracers. J Parasitol 68:253–258

Barrios-Ceballos MP, Martínez-Gallardo NA, Anaya-Velázquez F, Mirelman D, Padilla-Vaca F (2005) A novel protease from *Entamoeba histolytica* homologous to members of the family S28 of serine proteases. Exp Parasitol 110:270–275

Bruchhaus I, Loftus BJ, Hall N, Tannich E (2003) The intestinal protozoan parasite *Entamoeba histolytica* contains 20 cysteine protease genes, of which only a small subset is expressed during in vitro cultivation. Eukaryot Cell 2:501–509

Chávez-Munguía B, Cristóbal-Ramos AR, González-Robles A, Tsutsumi V, Martinez-Palomo A (2003) Ultrastructural study of *Entamoeba invadens* encystation and excystation. J Submicrosc Cytol Pathol 35:235–243

Chávez-Munguía B, Omaña-Molina M, González-Lázaro M, González-Robles A, Cedillo-Rivera R, Bonilla P, Martinez-Palomo A (2007) Ultrastructure of cyst differentiation in parasitic protozoa. Parasitol Res 100:1169–1175

Cleveland LR, Sanders EP (1930) Encystation, multiple fission without encystment, excystation, metacystic development, and variation in a pure line and nine strains of *Entamoeba histolytica*. Arch Protist 70:223–266

Diamond LS, Harlow DR, Cunnick CC (1978) A new medium for the axenic cultivation of *Entamoeba histolytica* and other *Entamoeba*. Trans R So Trop Med Hyg 72:431–432

Dobell C (1928) Researches on the intestinal protozoa of monkeys and man. Parasitology 20:357–412

Eichinger D (1997) Encystation of *Entamoeba* parasites. Bioessays 19:633–639

Felsenstein J (1985) Confidence limits on phylogenies: an approach using the bootstrap. Evolution 39:783–791

Frisardi M, Ghosh SK, Field J, Van Dellen K, Rogers R, Robbins P, Samuelson J (2000) The most abundant glycoprotein of amebic cyst walls (Jacob) is a lectin with five cys-rich, chitin-binding domains. Infect Immun 68:4217–4224

Garcia-Zapien AG, Hernandez-Gutierrez R, Mora-Galindo J (1995) Simultaneous growth and mass encystation of *Entamoeba invadens* under axenic conditions. Arch Med Res 26:257–262

Geiman QM, Ratcliffe HL (1936) Morphology and life-cycle of an amoeba producing amoebiasis in reptiles. Parasitology 28:208–230

Kanehisa M, Goto S (2000) KEGG: Kyoto encyclopedia of genes and genomes. Nucleic Acids Res 28:27–30

Keene WE, Petitt MG, Allen S, McKerrow JH (1986) The major neutral proteinase of *Entamoeba histolytica*. J Exp Med 163:536–549

Kumagai M, Kobayashi S, Okita T, Ohtomo H (2001) Modifications of Kohn's chlorazol black E staining and Wheatley's trichrome staining for temporary wet mount and permanent preparation of *Entamoeba histolytica*. J Parasitol 87:701–704

Laemmli UK (1970) Cleavage of structural proteins during the assembly of the head of bacteriophage T4. Nature 227:681–685

León G, Fiori C, Das P, Moreno M, Tovar R, Sánchez-Sala JL, Muñoz ML (1997) Electron probe analysis and biochemical characterization of electron-dense granules secreted by *Entamoeba histolytica*. Mol Biochem Res 85:233–242

López-Romero E, Villagómez-Castro JC (1993) Encystation in *Entamoeba invadens*. Parasitol Today 9:225–227

Makioka A, Kumagai M, Ohtomo H, Kobayashi S, Takeuchi T (2002) Effect of proteasome inhibitors on the growth, encystation, and excystation of *Entamoeba histolytica* and *Entamoeba invadens*. Parasitol Res 88:454–459

Makioka A, Kumagai M, Kobayashi S, Takeuchi T (2005) *Entamoeba invadens*: cysteine protease inhibitors block excystation and metacystic development. Exp Parasitol 109:27–32

McConnachie EW (1955) Studies on *Entamoeba invadens* Rodhain, 1934, in vitro, and its relationship to some other species of *Entamoeba*. Parasitol 45:452–481

McKerrow JH (1989) Parasite proteases. Exp Parasitol 68:111–115

Page RD (1996) TreeView: an application to display phylogenetic trees on personal computers. Comput Appl Biosci 12:357–358

Que X, Reed SL (2000) Cysteine proteinases and the pathogenesis of amebiasis. Clin Microbiol Rev 13:196–206

Rengpien S, Bailey GB (1975) Differentiation of *Entamoeba*: a new medium and optimal conditions for axenic encystation of *E. invadens*. J Parasitol 61:24–30

Riahi Y, Ankri S (2000) Involvement of serine proteases during encystation of *Entamoeba invadens*. Arch Med Res 31:S187–S189

Rosenthal PJ (1999) Proteases of protozoan parasites. Adv Parasitol 43:106–139

Saitou N, Nei M (1987) The neighbor-joining methods: a new method for reconstructing phylogenetic trees. Mol Biol Evol 4:406–425

Sajid M, McKerrow JH (2002) Cysteine proteases of parasitic organisms. Mol Biochem Parasitol 120:1–21

Sanchez L, Enea V, Eichinger D (1994) Identification of a developmentally regulated transcript expressed during encystation of *Entamoeba invadens*. Mol Biochem Parasitol 67:125–135

Thompson JD, Higgins DG, Gibson TJ (1994) CLUSTAL W: improving the sensitivity of progressive multiple sequence alignment through sequence weighting, position-specific gap penalties and weight matrix choice. Nucleic Acids Res 22:4673–4680

Tillack M, Biller L, Irmer H, Freitas M, Gomes MA, Tannich E, Bruchhaus I (2007) The *Entamoeba histolytica* genome: primary structure and expression of proteolytic enzymes. BMC Genomics 8:170–185

Yousef GM, Kopolovic AD, Elliott MB, Diamandis EP (2003) Genomic overview of serine proteases. Biochem Biophys Res Commun 305:28–36

Candida albicans keratitis modified by steroid application

Kaoru Araki-Sasaki[1]
Hiroko Sonoyama[1]
Tsutomu Kawasaki[1]
Nariyasu Kazama[1]
Hidenao Ideta[1]
Yoshitsugu Inoue[2]

[1]Ideta Eye Hospital, Kumamoto City, Kumamoto, Japan; [2]Department of Ophthalmology, Tottori University, Koyama-Minami, Tottori, Japan

Abstract: The paper reports on *Candida albicans* ocular infection modified by steroid eye drops. A 74-year-old male complained of conjunctival injection and pain in his right eye three months after pterygium and cataract surgery. After treatment with antibiotics and steroid eye drops for three days, he was referred to our hospital. Clear localized corneal endothelial plaque with injection of ciliary body was observed. No erosion of the corneal epithelium, or infiltration of stromal edema was observed, suggesting that the pathological organism derived from the intracameral region. Because ocular infection was suspected, steroid eye drops were stopped, which led immediately to typical infectious keratitis in the pathological region, with epithelial erosion, fluffy abscess, stromal infiltration, and edema. For diagnostic purposes, the plaque was surgically removed with forceps and the anterior chamber was irrigated with antibiotics. The smear and culture examination from the plaque revealed *C. albicans* surrounded by neutrophils. However, aqueous fluid and fibrous tissue after gonio procedure contained no mycotic organisms. Topical fluconazole, micafungin, and pimaricin with oral itraconazole (150 mg/day) were effective. Special attention is needed when prescribing steroid eye drops to treat corneal disease especially postoperatively. Diagnosing infectious keratitis is sometimes difficult because of modification by some factors, such as postoperative conditions, scarring, and drug-induced masking. Here, we report on mycotic keratitis modified by postoperative steroid administration.

Keywords: *Candida albicans*, cataract surgery, steroid, mycotic keratitis

Case report

A 74-year-old man underwent pterygium excision and cataract surgery at the same day in his right eye on June 2, 2006. At the time of cataract surgery (phacoemulsification), the posterior capsule was ruptured and anterior vitrectomy was performed before intraocular lens implant. 0.5% levofloxacin and 0.1% fluorometholone eye drops were applied for one month in the usual way. His corrected visual acuity was 0.5. On September 29, 2006, he suddenly complained of redness with a foreign body sensation in his right eye, and visited a general practitioner (GP), who prescribed 0.5% levofloxacin and 0.1% fluorometholone eye drops. Three days of treatment resolved the foreign body sensation, but the cilial injection continued, and he was referred to our hospital. Slit lamp examination disclosed clear corneal endothelial plaque and fibrous tissue in the anterior chamber with no remarkable corneal focus (Figure 1). Although the stromal opacity was recognized as the scar of the pterygium excision, stromal infiltrate and edema were not observed. The corneal epithelium was not eroded as if the pathogenic organism derived from the intracameral region. The patient was treated with 0.1% betamethasone sodium phosphate and 10 mg of oral predonisolone acetate with 0.5% levofloxacin eye drops for possible uveitis. Because no improvement was observed for a week, and infectious disease including postoperative endophthalmitis was suspected, 0.1% betamethasone sodium phosphate and 10 mg predonisolone acetate were discontinued. Instead, 0.1% levofloxacin was applied continuously. On the day after finishing steroid therapy, the typical appearance of mycotic keratitis, such

Correspondence: Kaoru Araki-Sasaki
Ideta Eye Hospital, 39, Nishi-tojincyo, Kumamoto City, 8600027, Kumamoto, Japan
Tel +81 96 325 5222
Fax +81 96 311 5512
Email sasakis@sa2.so-net.ne.jp

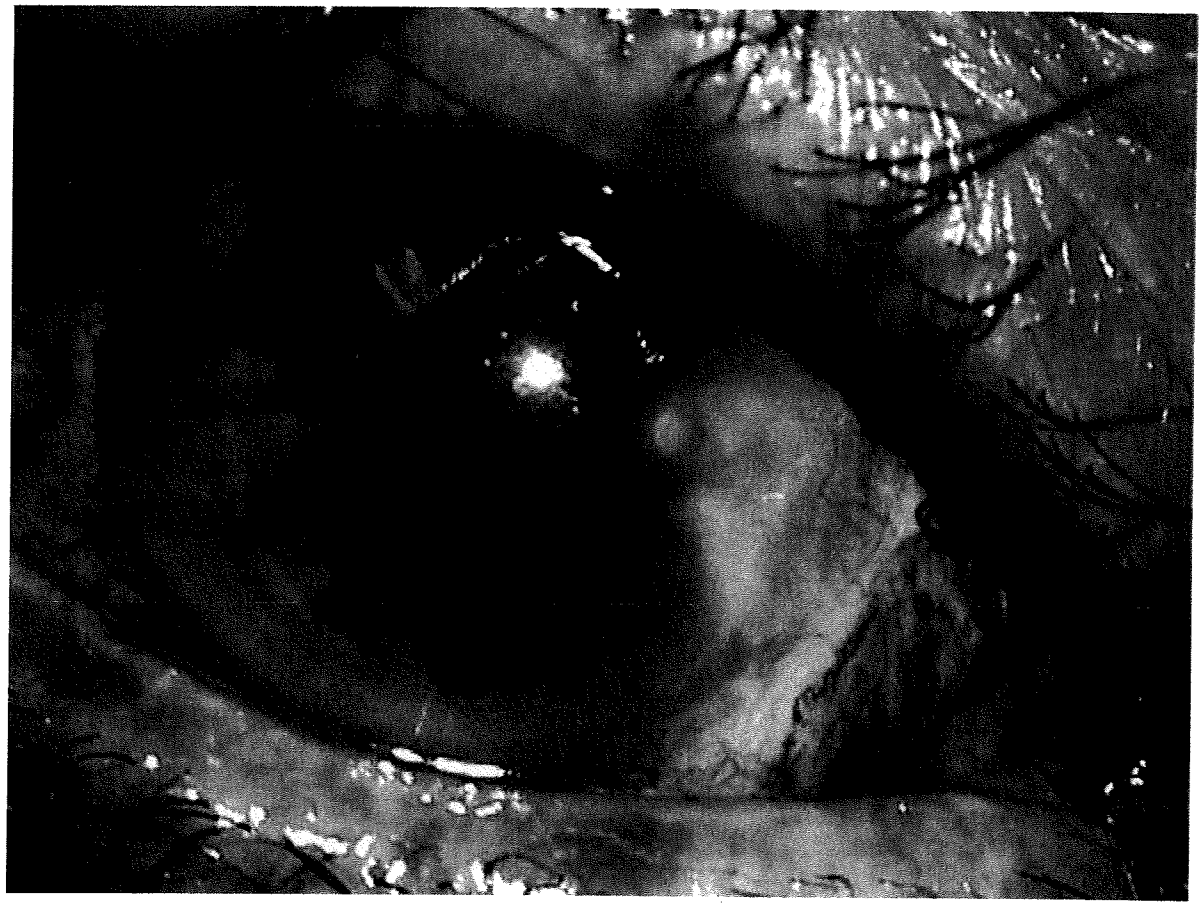

Figure 1 Clear corneal endothelial plaque was observed at the scar region of the excised pterygium.
Note: No remarkable stromal infiltration, no edema, and no epithelial defect.

as a stromal fluffy abcess with stromal infiltration and edema accompanied by endothelial plaque, was observed (Figure 2). Corneal epithelium was eroded and endothelial plaque enlarged with accumulation of hypopyon. For diagnostic purposes, the corneal endothelial plaque was surgically removed with forceps inserted from the limbus, followed by anterior chamber irrigation with calvapenem. The smear of the excised plaque disclosed yeast by Gram staining (Figure 2). *Candida albicans* was subsequently isolated by culture at Kumamoto City Medical Association Laboratory Center (Kumamoto, Japan). However, samples from aqueous humor and fibrous tissue at angulus iridocornealis were negative in culture. The minimum inhibitory concentration (MIC) of isolated *C. albicans* was fluconazole: <0.12, miconazole: <0.06, micafungin: <0.03, itraconazole: <0.015 μg/ml. 0.2% fluconazole, 0.2% micafungin eye drops hourly, and pimaricin ointment once daily with itraconazole (150 mg/day) orally were administered. Three weeks of antimycotic therapy resolved the mycotic keratitis and his visual acuity recovered to 0.7.

Comments

The clinical appearance of our patient was modified by steroid administration. Mycotic keratitis is often accompanied by a fluffy abscess with severe stromal edema and infiltration. Epithelial erosion and endothelial plaque with hypopyon are also characteristic of mycotic keratitis. Our patient showed clear endothelial plaque with no epithelial defect, no stromal infiltration, and no stromal edema at his first visit to our hospital as if the pathogenic organism derived intracamerally. Thus we first misdiagnosed it as uveitis or postoperative endophthalmitis. The mycotic organism may possibly have entered the eye during cataract surgery and become attached to the thinned retrocorneal region after pterygium surgery. The rupture of the posterior capsule during cataract surgery also makes diagnosis difficult, and raises the possibility